

Integral LQR Control of a Star-Shaped Octorotor

Victor G. ADÎR^{*1}, Adrian M. STOICA¹

^{*}Corresponding author

¹“POLITEHNICA” University of Bucharest, Faculty of Aerospace Engineering
Str. Gheorghe Polizu, nr. 1, sector 1, 011061, Bucharest, Romania
victor.adir@gmail.com

DOI: 10.13111/2066-8201.2012.4.2.1

Abstract: *The paper starts by presenting the model of the star-shaped octorotor. LQR control is chosen to stabilize the attitude and altitude of the vehicle. Waypoint navigation is also implemented. Numerical simulations demonstrate the effectiveness of the control strategy under nominal conditions. However, in practice mass related uncertainties can occur. In this case the results are unsatisfactory. Thus the improvement of the applied LQR control strategy is proposed. It is shown that after adding integral action to the altitude controller the issue is solved.*

Key Words: VTOL aircraft, autonomous UAV, octorotor, LQR control, integral action.

1. INTRODUCTION

Day by day quadrotor UAVs (unmanned aerial vehicles) are being used in more and more fields of activity. As their name suggests, they are powered by four rotors. Unlike conventional helicopters, they have fixed pitch propellers. Thus control is achieved by varying the speed of the rotors in order to induce the desired forces and moments. Although they are remarkable vehicles, some issues regarding their reliability and payload restrictions have to be considered. The quadrotor depends on all of the four rotors in order to provide full control. If even just one of them is completely inoperative then stabilization is impossible without reversing the direction of the motor or sacrificing the controllability of the yaw state, as seen in [1]. Octorotor configurations were proposed in [2] and [3]. The additional four rotors provide an increase in thrust, which translates into a higher payload capacity, and redundancy. The star-shaped octorotor (see [2]) is capable of VTOL (vertical take-off and landing) and it is highly manoeuvrable. It can be used for aerial imaging (remote monitoring of important points of interest, news coverage, commercials) and mapping (landscaping, agriculture), traffic surveillance, search and rescue operations, security missions and a lot more. Additionally, it can be deployed in environments which are dangerous for humans (highly toxic or radioactive, for example).

Section 2 presents the non-linear dynamic model of the star-shaped octorotor and its nominal parameters. In Section 3 a control strategy is proposed. Careful observation of the dynamics reveals the fact that the control problem can be separated into two parts - one for attitude control and one for position control. The model is simplified and some of the equations are linearized around the hover state. Section 4 presents the design of the LQR (Linear Quadratic Regulator) control laws (see for instance [6] and [7]). In Section 5 their effectiveness is tested using numerical simulations. As long as uncertainties are not present the desired results are achieved. However, in the case of mass related uncertainties problems appear. Thus in Section 6 integral action is added to the altitude controller (see for instance [4] and [5]). Testing confirms the correct approach has been taken. Conclusions and future developments are presented in Section 7.

2. DYNAMICS

The layout of the star-shaped octorotor is presented in Fig. 1. It consists of eight equal rods that are connected by a central plate which carries the avionics and power supply of the vehicle. There is a 45 degree angle between the neighbouring arms. The axis system is chosen to facilitate the transition from the quadrotor model. The standard definition of a positive rotation is used: this is defined as a counter-clockwise rotation around the axis as seen from directly in front of the axis line. Two reference frames are used – a body axes frame B fixed at the vehicle's centre of gravity and an earth fixed frame E.

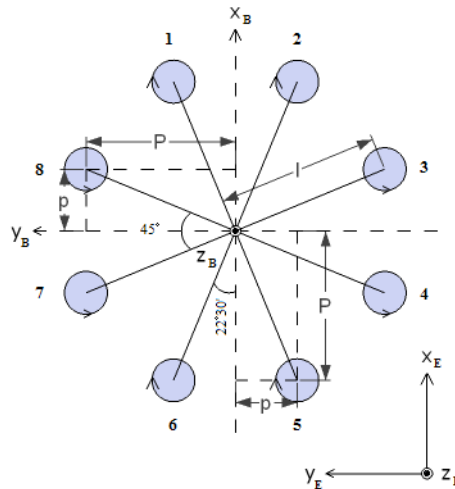


Fig. 1 – Star-shaped octorotor layout

In order to obtain a configuration similar to that of the quadrotor the actuators are paired together two by two in the following manner: pair A - 1 with 2 ($\Omega_1 = \Omega_2 = \Omega_A$), pair B - 3 with 4 ($\Omega_3 = \Omega_4 = \Omega_B$), pair C - 5 with 6 ($\Omega_5 = \Omega_6 = \Omega_C$) and pair D - 7 with 8 ($\Omega_7 = \Omega_8 = \Omega_D$). The rotors belonging to the same pair spin at the same speed and have propellers of the same type (either puller or pusher, depending on the direction of rotation).

To increase the roll angle, the thrust of pair B is decreased while the thrust of pair D is increased such that overall thrust remains the same. To obtain a positive pitch angle, the thrust of pair A is decreased while the thrust of pair C is simultaneously increased. For a positive yaw angle, the speed of the clockwise spinning rotors is increased while the speed of the counter-clockwise ones is decreased. The rotor arrows from Fig. 1 indicate the direction of the resulting torque which is opposite to the direction of rotation.

The dynamics of the star-shaped octorotor were derived taking into account the work on quadrotors which is presented in [6]-[12]. The following assumptions were made:

- the structure is rigid and symmetric
- the centre of gravity lies at the origin of the body axis reference frame
- the inertia matrix is diagonal
- the propellers are rigid
- actuator lag is considered negligible
- the thrust is proportional to the square of the speed of the rotor
- the drag is proportional to the square of the speed of the rotor

The equations describing the dynamics of the star-shaped octorotor are (as in the case of the quadrotor modelling presented in [10] and [12]):

$$\left\{ \begin{array}{l} \ddot{x} = (\cos \phi \sin \theta \cos \psi + \sin \phi \sin \psi) \frac{1}{m} U_4 \\ \ddot{y} = (\cos \phi \sin \theta \sin \psi - \sin \phi \cos \psi) \frac{1}{m} U_4 \\ \ddot{z} = -g + \cos \phi \cos \theta \frac{1}{m} U_4 \\ \dot{p} = q r \left(\frac{I_y - I_z}{I_x} \right) - \frac{J_r}{I_x} q \Omega + \frac{1}{I_x} U_1 \\ \dot{q} = p r \left(\frac{I_z - I_x}{I_y} \right) + \frac{J_r}{I_y} p \Omega + \frac{1}{I_y} U_2 \\ \dot{r} = p q \left(\frac{I_x - I_y}{I_z} \right) + \frac{1}{I_z} U_3. \end{array} \right. \quad (1)$$

The outputs of the system are x , y and z - which denote the position of the vehicle with respect to the Earth fixed frame, and p , q and r - which denote the angular velocity of the vehicle with respect to the body fixed frame. In order to obtain the angular velocity with respect to the Earth fixed frame the following multiplication is performed (see [13], [14]):

$$\begin{bmatrix} \dot{\phi} \\ \dot{\theta} \\ \dot{\psi} \end{bmatrix} = \begin{bmatrix} 1 & \sin \phi \tan \theta & \cos \phi \tan \theta \\ 0 & \cos \phi & -\sin \phi \\ 0 & \frac{\sin \phi}{\cos \theta} & \frac{\cos \phi}{\cos \theta} \end{bmatrix} \begin{bmatrix} p \\ q \\ r \end{bmatrix}. \quad (2)$$

The control inputs of the system, U_1 , U_2 , U_3 and U_4 , and the disturbance Ω (which depends on the speed of the rotors - Ω_1 , Ω_2 , Ω_3 , Ω_4 , Ω_5 , Ω_6 , Ω_7 and Ω_8) have the following expressions:

$$\left\{ \begin{array}{l} U_1 = b [P (\Omega_7^2 + \Omega_8^2 - \Omega_3^2 - \Omega_4^2) + p (\Omega_1^2 + \Omega_6^2 - \Omega_2^2 - \Omega_5^2)] \\ U_2 = b [P (\Omega_5^2 + \Omega_6^2 - \Omega_1^2 - \Omega_2^2) + p (\Omega_4^2 + \Omega_7^2 - \Omega_3^2 - \Omega_8^2)] \\ U_3 = d (\Omega_3^2 + \Omega_4^2 + \Omega_7^2 + \Omega_8^2 - \Omega_1^2 - \Omega_2^2 - \Omega_5^2 - \Omega_6^2) \\ U_4 = b (\Omega_1^2 + \Omega_2^2 + \Omega_3^2 + \Omega_4^2 + \Omega_5^2 + \Omega_6^2 + \Omega_7^2 + \Omega_8^2) \\ \Omega = \Omega_3 + \Omega_4 + \Omega_7 + \Omega_8 - \Omega_1 - \Omega_2 - \Omega_5 - \Omega_6. \end{array} \right. \quad (3)$$

where:

$$P = l \cos 22^\circ 30', \quad (4)$$

$$p = l \sin 22^\circ 30'. \quad (5)$$

Because of the pairing, some of the terms in equation set (3) cancel and therefore:

$$\begin{cases} U_1 = b[P(\Omega_7^2 + \Omega_8^2 - \Omega_3^2 - \Omega_4^2)] \\ U_2 = b[P(\Omega_5^2 + \Omega_6^2 - \Omega_1^2 - \Omega_2^2)] \\ U_3 = d(\Omega_3^2 + \Omega_4^2 + \Omega_7^2 + \Omega_8^2 - \Omega_1^2 - \Omega_2^2 - \Omega_5^2 - \Omega_6^2) \\ U_4 = b(\Omega_1^2 + \Omega_2^2 + \Omega_3^2 + \Omega_4^2 + \Omega_5^2 + \Omega_6^2 + \Omega_7^2 + \Omega_8^2) \\ \Omega = \Omega_3 + \Omega_4 + \Omega_7 + \Omega_8 - \Omega_1 - \Omega_2 - \Omega_5 - \Omega_6. \end{cases} \quad (6)$$

The inputs become:

$$\begin{cases} U_1 = 2b[P(\Omega_D^2 - \Omega_B^2)] \\ U_2 = 2b[P(\Omega_C^2 - \Omega_A^2)] \\ U_3 = 2d(\Omega_B^2 + \Omega_D^2 - \Omega_A^2 - \Omega_C^2) \\ U_4 = 2b(\Omega_A^2 + \Omega_B^2 + \Omega_C^2 + \Omega_D^2). \end{cases} \quad (7)$$

From equation set (7) it follows that:

$$\begin{cases} \Omega_1 = \Omega_2 = \Omega_A = \sqrt{-U_2/(4bP) - U_3/(8d) + U_4/(8b)} \\ \Omega_3 = \Omega_4 = \Omega_B = \sqrt{-U_1/(4bP) + U_3/(8d) + U_4/(8b)} \\ \Omega_5 = \Omega_6 = \Omega_C = \sqrt{U_2/(4bP) - U_3/(8d) + U_4/(8b)} \\ \Omega_7 = \Omega_8 = \Omega_D = \sqrt{U_1/(4bP) + U_3/(8d) + U_4/(8b)}. \end{cases} \quad (8)$$

The nominal parameters of the star-shaped octorotor are: $l = 0.4m$ - arm length, $m = 1.64kg$ - mass, $I_x = 0.044kg \cdot m^2$ - inertia on x axis, $I_y = 0.044kg \cdot m^2$ - inertia on y axis, $I_z = 0.088kg \cdot m^2$ - inertia on z axis, $b = 10 \cdot 10^{-6}N \cdot s^2$ - thrust coefficient, $d = 0.3 \cdot 10^{-6}N \cdot m \cdot s^2$ - drag coefficient and $J_r = 90 \cdot 10^{-6}kg \cdot m^2$ - rotor inertia.

3. MODELLING FOR CONTROL DESIGN

The design process can be simplified by modifying the dynamic model describing the behaviour of the vehicle as follows (see [2] and [6]-[10]):

$$\begin{cases} \ddot{x} = (\cos\phi \sin\theta \cos\psi + \sin\phi \sin\psi) \frac{1}{m} U_4 \\ \ddot{y} = (\cos\phi \sin\theta \sin\psi - \sin\phi \cos\psi) \frac{1}{m} U_4 \\ \ddot{z} = -g + \cos\phi \cos\theta \frac{1}{m} U_4 \\ \ddot{\phi} = \dot{\theta} \dot{\psi} \left(\frac{I_y - I_z}{I_x} \right) - \frac{J_r}{I_x} \dot{\theta} \Omega + \frac{1}{I_x} U_1 \\ \ddot{\theta} = \dot{\phi} \dot{\psi} \left(\frac{I_z - I_x}{I_y} \right) + \frac{J_r}{I_y} \dot{\phi} \Omega + \frac{1}{I_y} U_2 \\ \ddot{\psi} = \dot{\phi} \dot{\theta} \left(\frac{I_x - I_y}{I_z} \right) + \frac{1}{I_z} U_3. \end{cases} \quad (9)$$

This model is widely used in different research materials. This approximation is valid when perturbations from hover flight are small and $(\dot{\phi}, \dot{\theta}, \dot{\psi}) \approx (p, q, r)$.

Analysis of the simplified dynamics reveals the fact that the model can be split into two sub-systems: one for translation (x , y and z) and one for rotation (ϕ , θ and ψ). One notices that the angles and their time derivatives are independent of the translation components. However, the latter clearly depend on the rotation components. Thus the control structure presented in Fig. 2 is proposed. An altitude controller will provide U_4 which dictates overall thrust. The controller for the $x - y$ position will compute the desired roll and pitch angles depending on the desired values for x and y . These angles, along with the desired yaw angle, are fed into the attitude controller which provides U_1 , U_2 and U_3 .

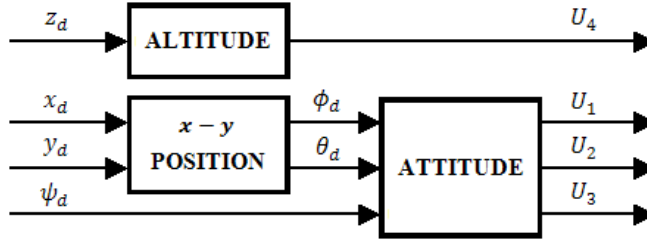


Fig. 2 – The proposed control structure

The following notations are introduced:

$$u_x = \cos \phi \sin \theta \cos \psi + \sin \phi \sin \psi, \quad (10)$$

$$u_y = \cos \phi \sin \theta \sin \psi - \sin \phi \cos \psi. \quad (11)$$

The control variables u_x and u_y can be regarded as virtual commands which rotate the thrust vector U_4 in such a way that the desired $x - y$ translation motion is achieved. Consider the system comprised of these two equations. If the values of u_x , u_y and ψ are provided then the two unknown parameters of this system can be determined. Thus one obtains the expressions for the desired roll and pitch angles:

$$\phi_d = \arcsin(\sin \psi u_x - \cos \psi u_y), \quad (12)$$

$$\theta_d = \arcsin\left(\frac{\cos \psi u_x + \sin \psi u_y}{\cos \phi_d}\right). \quad (13)$$

The following system comprises the attitude related equations of the simplified dynamic model presented in (9):

$$\begin{cases} \ddot{\phi} = \dot{\theta} \dot{\psi} \left(\frac{I_y - I_z}{I_x} \right) - \frac{J_r}{I_x} \dot{\theta} \Omega + \frac{1}{I_x} U_1 \\ \ddot{\theta} = \dot{\phi} \dot{\psi} \left(\frac{I_z - I_x}{I_y} \right) + \frac{J_r}{I_y} \dot{\phi} \Omega + \frac{1}{I_y} U_2 \\ \ddot{\psi} = \dot{\phi} \dot{\theta} \left(\frac{I_x - I_y}{I_z} \right) + \frac{1}{I_z} U_3. \end{cases} \quad (14)$$

This system is linearized around the hover state which corresponds to $\phi = \theta = \psi = 0 \text{ rad}$ and $\dot{\phi} = \dot{\theta} = \dot{\psi} = 0 \text{ rad / s}$. The result can be seen below:

$$\begin{cases} \ddot{\phi} = \frac{1}{I_x} U_1 \\ \ddot{\theta} = \frac{1}{I_y} U_2 \\ \ddot{\psi} = \frac{1}{I_z} U_3. \end{cases} \quad (15)$$

The following system, which is obtained from (9) by using (10) and (11), comprises the x and y position related equations of the simplified dynamic model:

$$\begin{cases} \ddot{x} = u_x \frac{1}{m} U_4 \\ \ddot{y} = u_y \frac{1}{m} U_4. \end{cases} \quad (16)$$

However:

$$\ddot{z} = -g + \cos \phi \cos \theta \frac{1}{m} U_4, \quad (17)$$

where the control variable U_4 (thrust related) must be determined in order to stabilize the above dynamics and to track a constant reference denoted by z_d . $\phi = \theta = \psi = 0 \text{ rad}$ at hover. Thus:

$$\ddot{z} = -g + \frac{1}{m} U_4. \quad (18)$$

Moreover, at hover $\ddot{z} = 0$. It follows that:

$$\frac{1}{m} U_4 = g, \quad (19)$$

which gives:

$$U_4 = m g. \quad (20)$$

Thus the previously presented system is adjusted to the corresponding hover state:

$$\begin{cases} \ddot{x} = u_x g \\ \ddot{y} = u_y g. \end{cases} \quad (21)$$

In regard to the altitude related equation of the simplified dynamic model (9), the following virtual control input is introduced:

$$u_z = -g + \cos \phi \cos \theta \frac{1}{m} U_4 \quad (22)$$

and thus:

$$\ddot{z} = u_z. \quad (23)$$

However, u_z is just a virtual control input. Thus, by replacing u_z in equation (17), the real control input is obtained:

$$U_4 = \frac{m(u_z + g)}{\cos \phi \cos \theta}. \quad (24)$$

The simplified dynamic model becomes:

$$\begin{cases} \ddot{x} = u_x g \\ \ddot{y} = u_y g \\ \ddot{z} = u_z \\ \ddot{\phi} = U_1 / I_x \\ \ddot{\theta} = U_2 / I_y \\ \ddot{\psi} = U_3 / I_z \end{cases} \quad (25)$$

The state vector is chosen as:

$$X^T = [x_1 \ x_2 \ x_3 \ x_4 \ x_5 \ x_6 \ x_7 \ x_8 \ x_9 \ x_{10} \ x_{11} \ x_{12}]^T, \quad (26)$$

namely:

$$X^T = [x \ \dot{x} \ y \ \dot{y} \ z \ \dot{z} \ \phi \ \dot{\phi} \ \theta \ \dot{\theta} \ \psi \ \dot{\psi}]^T. \quad (27)$$

4. LQR CONTROLLER DESIGN

a) Attitude Control

Let us define the attitude state vector as:

$$X_a = \begin{bmatrix} x_7 \\ x_8 \\ x_9 \\ x_{10} \\ x_{11} \\ x_{12} \end{bmatrix} = \begin{bmatrix} \phi \\ \dot{\phi} \\ \theta \\ \dot{\theta} \\ \psi \\ \dot{\psi} \end{bmatrix} = \begin{bmatrix} x_7 \\ \dot{x}_7 \\ x_9 \\ \dot{x}_9 \\ x_{11} \\ \dot{x}_{11} \end{bmatrix}. \quad (28)$$

Then the attitude system can be written in state space form as follows:

$$\begin{bmatrix} \dot{x}_7 \\ \dot{x}_8 \\ \dot{x}_9 \\ \dot{x}_{10} \\ \dot{x}_{11} \\ \dot{x}_{12} \end{bmatrix} = \begin{bmatrix} 0 & 1 & 0 & 0 & 0 & 0 \\ 0 & 0 & 0 & 0 & 0 & 0 \\ 0 & 0 & 0 & 1 & 0 & 0 \\ 0 & 0 & 0 & 0 & 0 & 0 \\ 0 & 0 & 0 & 0 & 0 & 1 \\ 0 & 0 & 0 & 0 & 0 & 0 \end{bmatrix} \begin{bmatrix} x_7 \\ x_8 \\ x_9 \\ x_{10} \\ x_{11} \\ x_{12} \end{bmatrix} + \begin{bmatrix} 0 & 0 & 0 \\ 1/I_x & 0 & 0 \\ 0 & 0 & 0 \\ 0 & 1/I_y & 0 \\ 0 & 0 & 0 \\ 0 & 0 & 1/I_z \end{bmatrix} \begin{bmatrix} U_1 \\ U_2 \\ U_3 \end{bmatrix}, \quad (29)$$

where:

$$A = \begin{bmatrix} 0 & 1 & 0 & 0 & 0 & 0 \\ 0 & 0 & 0 & 0 & 0 & 0 \\ 0 & 0 & 0 & 1 & 0 & 0 \\ 0 & 0 & 0 & 0 & 0 & 0 \\ 0 & 0 & 0 & 0 & 0 & 1 \\ 0 & 0 & 0 & 0 & 0 & 0 \end{bmatrix} \quad (30)$$

and:

$$B = \begin{bmatrix} 0 & 0 & 0 \\ 1/I_x & 0 & 0 \\ 0 & 0 & 0 \\ 0 & 1/I_y & 0 \\ 0 & 0 & 0 \\ 0 & 0 & 1/I_z \end{bmatrix} \quad (31)$$

denote the state matrix and the input matrix, respectively, and $U = [U_1 \ U_2 \ U_3]^T$ denotes the input vector. Given the continuous-time linear system $\dot{X}_a = A X_a + B U$ the aim is to find the stabilizing feedback control law $U = -K X_a$ that minimizes the following cost function:

$$J = \int_0^\infty (X_a^T Q X_a + U^T R U) dt, \quad (32)$$

where $Q \geq 0$ and $R > 0$ are weighting matrices of appropriate dimensions. The first term corresponds to the energy of the controlled output, while the second term corresponds to the energy of the control signal. Thus, depending on the desired performance and the available capabilities, the choice of the Q and R matrices is an important issue. As a starting point, Bryson's rule can be applied (see for instance [15]). Afterwards, the matrices can be refined through a trial-and-error iterative process until the desired response characteristics are obtained. Bryson's rule states that Q and R can be chosen diagonal as follows:

$$Q_{i,i} = \frac{1}{\text{maximum acceptable value of } X_{a_i}^2}, i = \overline{1,6}, \quad (33)$$

$$R_{j,j} = \frac{1}{\text{maximum acceptable value of } U_j^2}, j = \overline{1,3}. \quad (34)$$

K is defined as:

$$K = R^{-1} B^T P, \quad (35)$$

while P denotes the stabilizing solution of the algebraic Riccati equation:

$$A^T P + P A - P B R^{-1} B^T P + Q = 0. \quad (36)$$

When desired state values (X_{a_d}) are imposed, the feedback control law takes the form:

$$U = -K (X_a - X_{a_d}). \quad (37)$$

Remark 1. The above control law used for tracking essentially exploits the expression of the state matrix A derived above. Indeed, assuming that the desired state vector X_{a_d} is constant and satisfies the condition:

$$\dot{X}_{a_d} = A X_{a_d}, \quad (38)$$

by subtracting the above equation from equation (29) one obtains:

$$\dot{e} = A e + B U, \quad (39)$$

where $e = X_a - X_{a_d}$ denotes the tracking error. Then the solution of the linear quadratic problem for the above system is just $U = -K (X_a - X_{a_d})$. Let us notice that the condition $\dot{X}_{a_d} = A X_{a_d}$ is fulfilled if $X_{a_d} = [\phi_d \ 0 \ \theta_d \ 0 \ \psi_d \ 0]^T$ with ϕ_d , θ_d and ψ_d assumed constant. For a more general case when the condition $\dot{X}_{a_d} = A X_{a_d}$ is not accomplished one

can see for instance [16], [17] and their references. After applying the iterative trial-and-error design procedure the following form for the Q and R matrices is reached:

$$Q = \begin{bmatrix} 7.5 & 0 & 0 & 0 & 0 & 0 \\ 0 & 1 & 0 & 0 & 0 & 0 \\ 0 & 0 & 7.5 & 0 & 0 & 0 \\ 0 & 0 & 0 & 1 & 0 & 0 \\ 0 & 0 & 0 & 0 & 35 & 0 \\ 0 & 0 & 0 & 0 & 0 & 5 \end{bmatrix}, \quad (40)$$

$$R = \begin{bmatrix} 0.05 & 0 & 0 \\ 0 & 0.05 & 0 \\ 0 & 0 & 0.025 \end{bmatrix}, \quad (41)$$

After computing the solution of the algebraic Riccati equation and replacing in the corresponding formula K is found to be:

$$K = \begin{bmatrix} 12.2474 & 4.5911 & 0 & 0 & 0 & 0 \\ 0 & 0 & 12.2474 & 4.5911 & 0 & 0 \\ 0 & 0 & 0 & 0 & 37.4166 & 14.3731 \end{bmatrix}. \quad (42)$$

b) Altitude Control

In this case the state vector is chosen as:

$$X_z = \begin{bmatrix} x_5 \\ x_6 \end{bmatrix} = \begin{bmatrix} z \\ \dot{z} \end{bmatrix} = \begin{bmatrix} x_5 \\ \dot{x}_5 \end{bmatrix} \quad (43)$$

and then the system is written in state space form as follows:

$$\begin{bmatrix} \dot{x}_5 \\ \dot{x}_6 \end{bmatrix} = \begin{bmatrix} 0 & 1 \\ 0 & 0 \end{bmatrix} \begin{bmatrix} x_5 \\ x_6 \end{bmatrix} + \begin{bmatrix} 0 \\ 1 \end{bmatrix} u_z, \quad (44)$$

where $A_z = \begin{bmatrix} 0 & 1 \\ 0 & 0 \end{bmatrix}$ is the state matrix, $B_z = \begin{bmatrix} 0 \\ 1 \end{bmatrix}$ denotes the input matrix and u_z is the input. Given the continuous-time linear system $\dot{X}_z = A_z X_z + B_z u_z$ the aim is to find the stabilizing feedback control law $u_z = -K_z X_z$ that minimizes the following cost function:

$$J_z = \int_0^\infty (X_z^T Q_z X_z + u_z^T R_z u_z) dt, \quad (45)$$

where $Q_z \geq 0$ and $R_z > 0$ are weighting matrices of appropriate dimensions. K_z is defined as:

$$K_z = R_z^{-1} B_z^T P_z, \quad (46)$$

while P_z stands for the stabilizing solution of the algebraic Riccati equation:

$$A_z^T P_z + P_z A_z - P_z B_z R_z^{-1} B_z^T P_z + Q_z = 0. \quad (47)$$

When desired state values (X_{z_d}) are imposed, the feedback control law takes the form (see Remark 1 from 4.a):

$$u_z = -K_z (X_z - X_{z_d}). \quad (48)$$

After applying the iterative trial-and-error design procedure the following form for the Q_z and R_z matrices is reached:

$$Q_z = \begin{bmatrix} 1 & 0 \\ 0 & 1 \end{bmatrix}, \quad (49)$$

$$R_z = 0.1. \quad (50)$$

After computing the stabilizing solution of the algebraic Riccati equation and replacing in the corresponding formula K_z is found to be:

$$K_z = [3.1623 \ 4.0404]. \quad (51)$$

c) Position Control on the x and y axes

For the position control on the x and y axes the state vector is chosen as:

$$X_{xy} = \begin{bmatrix} x_1 \\ x_2 \\ x_3 \\ x_4 \end{bmatrix} = \begin{bmatrix} x \\ \dot{x} \\ y \\ \dot{y} \end{bmatrix} = \begin{bmatrix} x_1 \\ \dot{x}_1 \\ x_3 \\ \dot{x}_3 \end{bmatrix}. \quad (52)$$

The corresponding state space equations are:

$$\begin{bmatrix} \dot{x}_1 \\ \dot{x}_2 \\ \dot{x}_3 \\ \dot{x}_4 \end{bmatrix} = \begin{bmatrix} 0 & 1 & 0 & 0 \\ 0 & 0 & 0 & 0 \\ 0 & 0 & 0 & 1 \\ 0 & 0 & 0 & 0 \end{bmatrix} \begin{bmatrix} x_1 \\ x_2 \\ x_3 \\ x_4 \end{bmatrix} + \begin{bmatrix} 0 & 0 \\ g & 0 \\ 0 & 0 \\ 0 & g \end{bmatrix} \begin{bmatrix} u_x \\ u_y \end{bmatrix}, \quad (53)$$

where $A_{xy} = \begin{bmatrix} 0 & 1 & 0 & 0 \\ 0 & 0 & 0 & 0 \\ 0 & 0 & 0 & 1 \\ 0 & 0 & 0 & 0 \end{bmatrix}$ is the state matrix, $B_{xy} = \begin{bmatrix} 0 & 0 \\ g & 0 \\ 0 & 0 \\ 0 & g \end{bmatrix}$ is the input matrix and $U_{xy} = \begin{bmatrix} u_x \\ u_y \end{bmatrix}$

is the input vector. For the continuous-time linear system $\dot{X}_{xy} = A_{xy} X_{xy} + B_{xy} U_{xy}$ the optimal control problem consists of finding the stabilizing feedback control law $U_{xy} = -K_{xy} X_{xy}$ that minimizes the following cost function:

$$J_{xy} = \int_0^\infty (X_{xy}^T Q_{xy} X_{xy} + U_{xy}^T R_{xy} U_{xy}) dt, \quad (54)$$

where $Q_{xy} \geq 0$ and $R_{xy} > 0$ are weighting matrices of appropriate dimensions. K_{xy} is defined as:

$$K_{xy} = R_{xy}^{-1} B_{xy}^T P_{xy}, \quad (55)$$

while P_{xy} is obtained by solving the continuous-time algebraic Riccati equation:

$$A_{xy}^T P_{xy} + P_{xy} A_{xy} - P_{xy} B_{xy} R_{xy}^{-1} B_{xy}^T P_{xy} + Q_{xy} = 0. \quad (56)$$

When desired state values (X_{xy_d}) are constant, based on a similar reasoning as in Remark 1 (see 4.a), the feedback control law takes the form:

$$U_{xy} = -K_{xy} (X_{xy} - X_{xy_d}). \quad (57)$$

After applying the iterative trial-and-error design procedure the following form for the Q_{xy} and R_{xy} matrices is reached:

$$Q_{xy} = \begin{bmatrix} 0.125 & 0 & 0 & 0 \\ 0 & 0.25 & 0 & 0 \\ 0 & 0 & 0.125 & 0 \\ 0 & 0 & 0 & 0.25 \end{bmatrix}, \quad (58)$$

$$R_{xy} = \begin{bmatrix} 2 & 0 \\ 0 & 2 \end{bmatrix}. \quad (59)$$

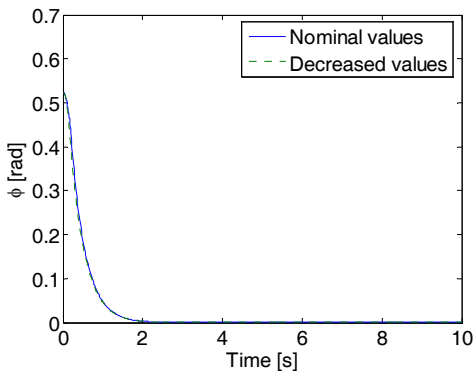
After computing the stabilizing solution of the algebraic Riccati equation and replacing in the corresponding formula K_{xy} is found to be:

$$K_{xy} = \begin{bmatrix} 0.2500 & 0.4195 & 0 & 0 \\ 0 & 0 & 0.2500 & 0.4195 \end{bmatrix}. \quad (60)$$

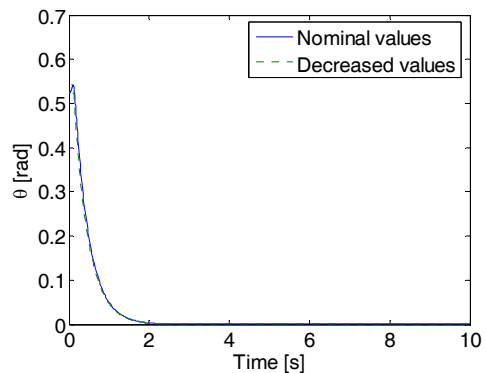
5. NUMERICAL SIMULATIONS FOR THE LQR CONTROLLER

The dynamics of the star-shaped octorotor is simulated using the proper model presented in (1). The true capabilities of the actuators are taken into consideration, as saturation may affect the control process. The simplified model described in equation set (9) is only used as the starting point for designing the control laws. For all test scenarios the star-shaped octorotor starts from the origin being tilted by 30 degrees on all three axes. The first test investigates the vehicle's ability to hover. In order to provide support for human control it needs to stabilize itself automatically. One easily observes from Fig. 3 that the target altitude of 20 metres is reached around $t = 6$ s, while the roll and pitch angles are stabilized before $t = 2$ s. The desired yaw value is obtained around $t = 2.5$ s. In the second test the mass and mass-related parameters of the vehicle are considered to be 20% lower than their nominal values. In practice this can happen when using a lighter battery, for example. The star-shaped octorotor has to perform the same task as in the first scenario. For easy comparison the time responses are plotted against each other in Fig. 3.

The effect produced by changing the inertia coefficients of the star-shaped octorotor is barely noticeable in the case of the attitude stabilization. However, regarding altitude control, a steady state error is present. The impact on the altitude controller is greater than the one noticed in the case of attitude control. The magnitude of the involved coefficients can provide hints about the way they affect the behaviour of the vehicle.



a) Roll angle



b) Pitch angle

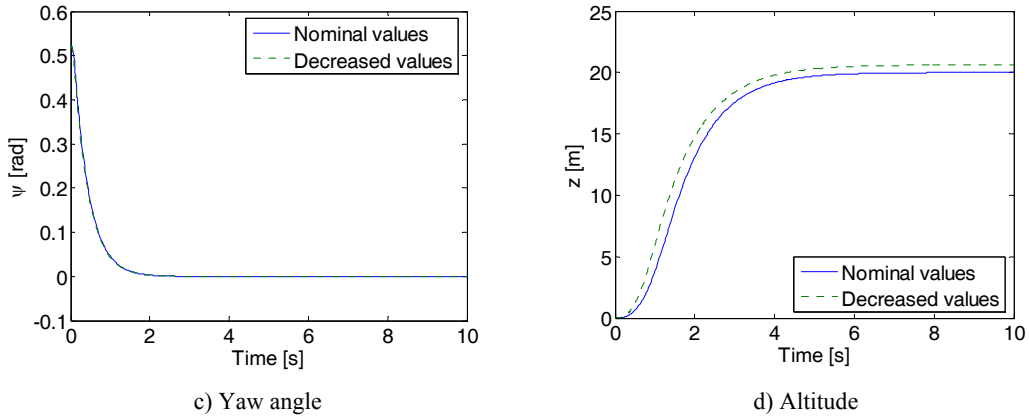
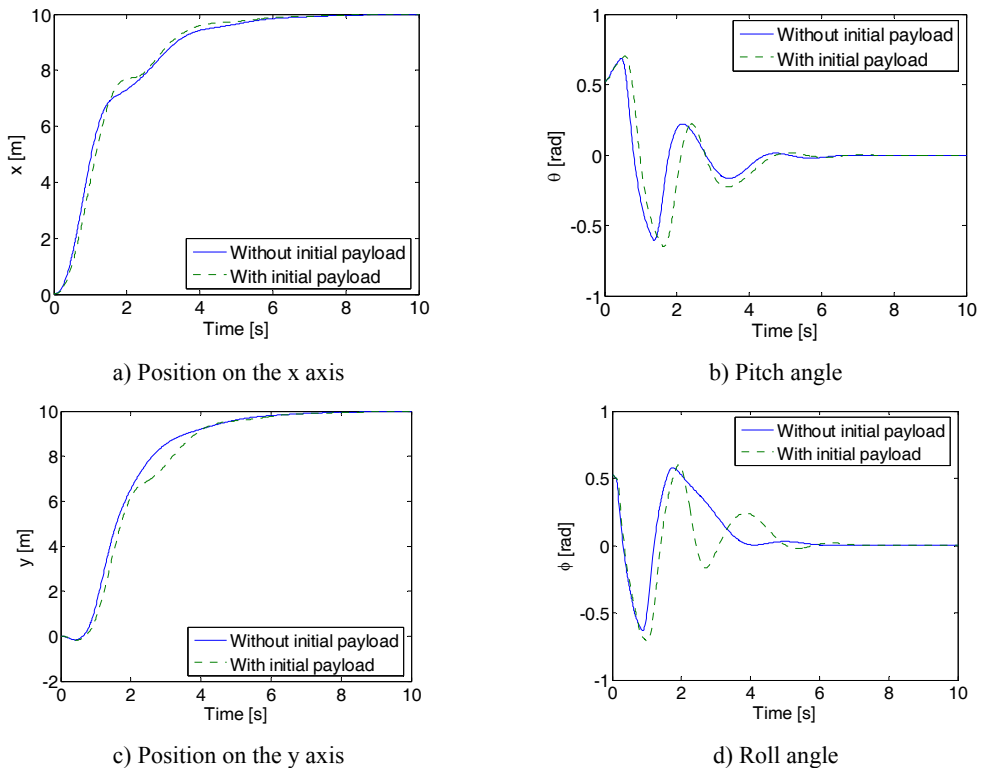


Fig. 3 Time responses for the first and second scenarios

The third test deals with the vehicle's ability to carry objects. It is assumed that an item attached to the star-shaped octorotor causes an increase of the mass and mass-related parameters by 30%. The vehicle drops the object at $t = 6\text{ s}$. Thus the previously mentioned parameters return to their nominal values.

During this test the vehicle has to navigate to the waypoint defined by (10,10,20) while maintaining a stable yaw angle of 0 degrees.

As seen in Fig. 4, the vehicle can handle the additional weight. However, this load has a major impact especially on altitude control. The decrease in performance is noticeable when compared to the payload-free case.



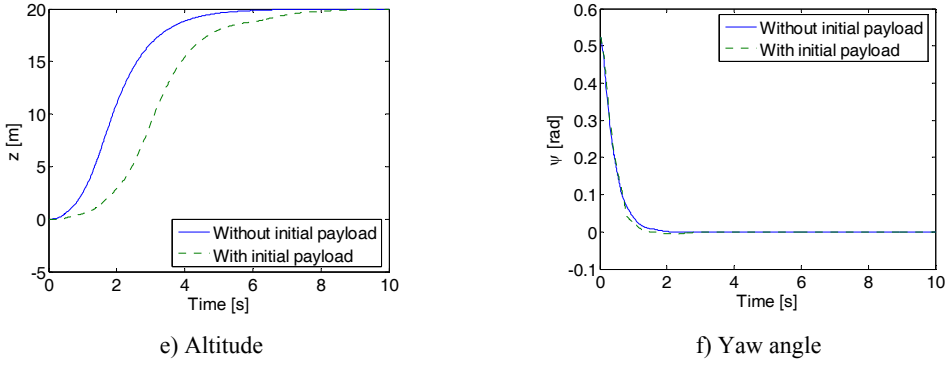


Fig. 4 Time responses for the third scenario

Having the ability to carry a variable payload is an important feature. In the next section which is dedicated to integral action the LQR controller for altitude will be developed in order to properly accommodate for this issue.

6. AUGMENTATION OF THE ALTITUDE CONTROLLER

The integral action in a control configuration is required in order to ensure the tracking of a constant reference (see [4], [5] and [16]). Before using this approach for the altitude control of the star-shaped octorotor some remarks should be emphasized. Consider the linear system:

$$\dot{x} = Ax + Bu, \quad (61)$$

where the pair (A, B) is assumed to be controllable, and the regulated output:

$$z = Cx. \quad (62)$$

Let the tracking error of a constant reference r be defined as:

$$e = Cx - r. \quad (63)$$

Then the augmented system with integral action has the state space equations:

$$\dot{x} = Ax + Bu \quad (64)$$

$$\dot{z} = Cx \quad (65)$$

or equivalently,

$$\dot{x}_a = A_a x_a + B_a u, \quad (66)$$

where $x_a = [x^T \ z^T]^T$, $A_a = \begin{bmatrix} A & 0 \\ C & 0 \end{bmatrix}$ and $B_a = \begin{bmatrix} B \\ 0 \end{bmatrix}$. The solution of the linear quadratic problem associated with the augmented system is given by:

$$u = -R_a^{-1} B_a^T P_a x_a, \quad (67)$$

where P_a denotes the stabilizing solution of the algebraic Riccati equation:

$$A_a^T P_a + P_a A_a - P_a B_a R_a^{-1} B_a^T P_a + Q_a = 0, \quad (68)$$

where $Q_a \geq 0$ and $R_a > 0$ are weighting matrices for the augmented state x_a and for the control u , respectively. Let us notice that in the case when the system (A, B, C) has transmission zeros in the origin then the pair (A_a, B_a) may become uncontrollable, thus the control problem having no solution (see [21]). In fact, a similar assumption, namely the fact that the transmission zeros of (A, B, C) must not coincide with the poles of the intern model

($1/s$ in our case), is made in [18]. In the following developments the subscript “ a ” will be removed for simplicity of writing. Let $\dot{x}_{5i} = e_5$, where $e_5 = x_5 - x_{5d}$. For a constant reference x_{5d} it follows that $\dot{e}_5 = \dot{x}_5$. The augmented state vector is in this case:

$$X_z = \begin{bmatrix} e_5 \\ x_6 \\ x_{5i} \end{bmatrix} = \begin{bmatrix} e_5 \\ \dot{x}_5 \\ x_{5i} \end{bmatrix} = \begin{bmatrix} x_5 - x_{5d} \\ \dot{z} \\ \int_0^t e_5(\tau) d\tau \end{bmatrix}. \quad (69)$$

The system can be written in state space form as follows:

$$\begin{bmatrix} \dot{e}_5 \\ \dot{x}_6 \\ \dot{x}_{5i} \end{bmatrix} = \begin{bmatrix} 0 & 1 & 0 \\ 0 & 0 & 0 \\ 1 & 0 & 0 \end{bmatrix} \begin{bmatrix} e_5 \\ x_6 \\ x_{5i} \end{bmatrix} + \begin{bmatrix} 0 \\ 1 \\ 0 \end{bmatrix} u_z, \quad (70)$$

where:

$$A_z = \begin{bmatrix} 0 & 1 & 0 \\ 0 & 0 & 0 \\ 1 & 0 & 0 \end{bmatrix} \quad (71)$$

and:

$$B_z = \begin{bmatrix} 0 \\ 1 \\ 0 \end{bmatrix} \quad (72)$$

denote the state matrix and the input matrix, respectively and u_z is the control variable.

Given the continuous-time linear system $\dot{X}_z = A_z X_z + B_z u_z$ the aim is to find the feedback control law $u_z = -K_z X_z$ that minimizes the following cost function:

$$J_z = \int_0^\infty (X_z^T Q_z X_z + u_z^T R_z u_z) dt, \quad (73)$$

K_z being given by:

$$K_z = R_z^{-1} B_z^T P_z, \quad (74)$$

while P_z is the stabilizing solution of the continuous-time algebraic Riccati equation:

$$A_z^T P_z + P_z A_z - P_z B_z R_z^{-1} B_z^T P_z + Q_z = 0. \quad (75)$$

After applying the iterative trial-and-error design procedure the following form for the Q_z and R_z matrices is reached:

$$Q_z = \begin{bmatrix} 9.5 & 0 & 0 \\ 0 & 5.5 & 0 \\ 0 & 0 & 0.000025 \end{bmatrix}, \quad (76)$$

$$R_z = 0.1. \quad (77)$$

After computing the stabilizing solution of the algebraic Riccati equation and replacing in the corresponding formula K_z is found to be:

$$K_z = [9.7608 \quad 8.6326 \quad 0.0158]. \quad (78)$$

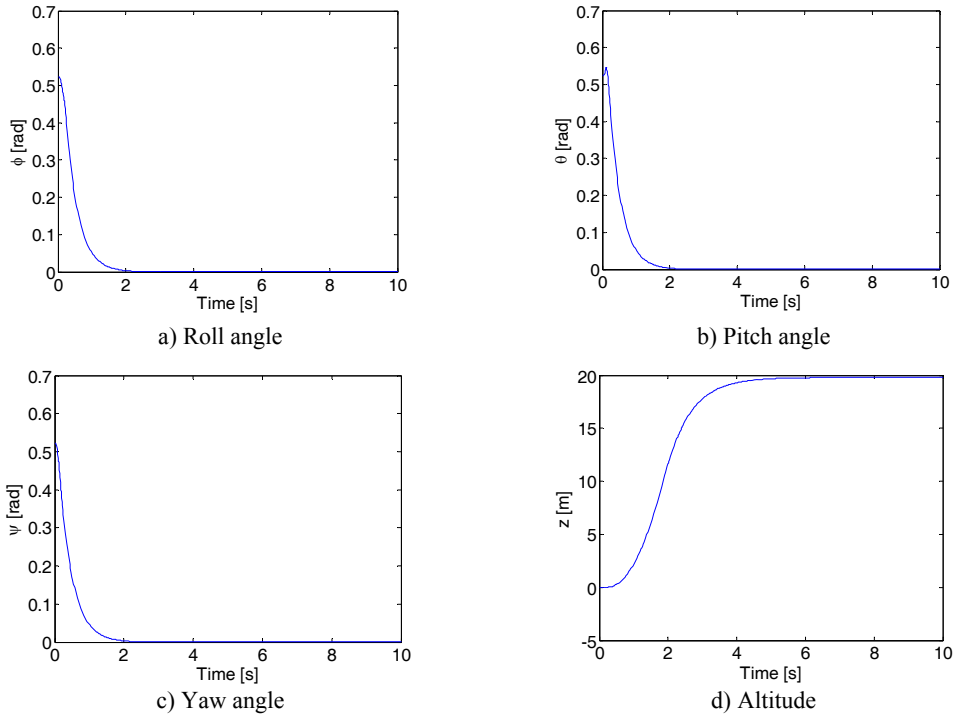


Fig. 5 Time responses for the fourth scenario

The fourth scenario assumes a 20% increase of the mass and mass related parameters. The vehicle has to stabilize its attitude and reach an altitude of 20 metres. The same initial conditions which were used for the previous simulations are considered. The target altitude is reached around $t = 5.5$ s, while the attitude is stabilized before $t = 2$ s.

Thus the results presented in Fig. 5 demonstrate the controller's ability to cope with the mass related uncertainty.

7. CONCLUSIONS AND FUTURE DEVELOPMENTS

The LQR methodology was used to design controllers for the attitude and position of the star-shaped octorotor. Numerical simulations were carried out using the non-linear dynamic model of the vehicle. Multiple scenarios were considered. Under nominal conditions the controllers proved to be effective.

However, in the case of mass related uncertainty altitude control was not precise. In practice this can easily occur by adding or removing equipment depending on the mission objectives.

For example, a video camera can be installed. An autonomous UAV should overcome such uncertainties.

Thus adding integral action to the LQR altitude controller was proposed. This approach provided the desired results and it should be extended to the other controllers as this should result in better performance in the case of uncertainties.

Future work focuses on applying non-linear control techniques like integral backstepping and integral sliding mode on the star-shaped octorotor (see [19] and [20]). The investigation of fault tolerant controllers is also considered (see [12]).

ACKNOWLEDGEMENTS

The work of Victor Adîr has been funded by the Sectoral Operational Programme Human Resources Development 2007-2013 of the Romanian Ministry of Labour, Family and Social Protection through the Financial Agreement POSDRU/6/1.5/S/19.

REFERENCES

- [1] Alessandro Freddi, Alexander Lanzon and Sauro Longhi, *A Feedback Linearization Approach to Fault Tolerance in Quadrotor Vehicles*, Preprints of the 18th IFAC World Congress, pp. 5413-5418, Milano (Italy), August 28 - September 2, 2011.
- [2] Victor G. Adîr, Adrian M. Stoica and James F. Whidborne, *Modelling and Control of a Star-shaped Octorotor*, International Conference on Mechanical Engineering, Robotics and Aerospace (ICMERA 2011), pp. 195-199, Romania, 2011.
- [3] V. G. Adîr, A. M. Stoica, A. Marks and J. F. Whidborne, *Modelling, stabilization and single motor failure recovery of a 4Y octorotor*, Proceedings of the IASTED International Conference of Intelligent Systems and Control (ISC 2011), pp. 82 – 87, Cambridge, United Kingdom, July 2011.
- [4] Graham C. Goodwin, Stefan F. Graebe and Mario E. Salgado, *Control System Design*, Prentice Hall, 2001.
- [5] Hamid Teimoori, Hemanshu R. Pota, Matt Garratt and Mahendra K. Samal, *Planar Trajectory Tracking Controller For a Small-sized Helicopter Considering Servos and Delay Constraints*, 37th Annual Conference of the IEEE Industrial Electronics Society, pp. 629-634, Melbourne, Australia, October 2011.
- [6] S. Bouabdallah, *Design and Control of Quadrotors with Applications to Autonomous Flying*, PhD Thesis, Ecole Polytechnique Federale de Lausanne, 2007.
- [7] S. Bouabdallah, A. Noth and R. Siegwart, *PID vs LQ control techniques applied to an indoor micro quadrotor*, Proceedings of 2004 IEEE/RSJ International Conference on Intelligent Robots and Systems (IROS 2004), vol. 3, pp. 2451 – 2456, Sendai, Japan, October 2004.
- [8] S. Bouabdallah, P. Murrieri and R. Siegwart, *Design and control of an indoor micro quadrotor*, Proceedings of the 2004 IEEE International Conference on Robotics and Automation (ICRA '04), vol. 5, pp. 4393 – 4398, New Orleans, LA, April 2004.
- [9] S. Bouabdallah and R. Siegwart, *Backstepping and sliding-mode techniques applied to an indoor micro quadrotor*, Proceedings of the 2005 IEEE International Conference on Robotics and Automation (ICRA '05), pp. 2247 – 2252, Barcelona, Spain, April 2005.
- [10] Tommaso Bresciani, *Modelling, Identification and Control of a Quadrotor Helicopter*, MSc Thesis, Lund University, 2008.
- [11] Ian Cowling, *Towards Autonomy of a Quadrotor UAV*, PhD Thesis, Cranfield University, 2008.
- [12] Youmin Zhang and Abbas Chamseddine, *Fault Tolerant Flight Control Techniques with Application to a Quadrotor UAV Testbed*, *Automatic Flight Control Systems-Latest Developments*, InTech, January 2012.
- [13] T. V. Chelaru, *Dinamica Zborului – Note de curs*, POLITEHNICA PRESS, Bucureşti, 2009.
- [14] T. V. Chelaru, *Dirijarea aparatelor de zbor – Note de curs*, POLITEHNICA PRESS, Bucureşti, 2009.
- [15] Jorge Miguel Brito Domingues, *Quadrotor prototype*, Master's Thesis, Instituto Superior Técnico, Universidade Técnica de Lisboa, 2009.
- [16] K. P. Groves, D. O. Sigthorsson, A. Serrani, S. Yurkovich, M. A. Bolender and D. B. Doman, *Reference Command Tracking for a Linearized Model of an Air-breathing Hypersonic Vehicle*, Proceedings of the AIAA Guidance, Navigation, and Control Conference and Exhibit, San Francisco, California, 15 - 18 August 2005.
- [17] Rocio Alba-Flores, Enrique Barbieri, *Real-time Infinite Horizon Linear-Quadratic Tracking Controller for Vibration Quenching in Flexible Beams*, Proceedings of the IEEE Conference on Systems, Man, and Cybernetics, Taipei, Taiwan, October 8-11, 2006.
- [18] E.J. Davison, A.G. Goldenberg, *Robust Control of a General Servomechanism Problem: The Servo Compensator*, *Automatica*, vol. 11, pp. 461-471, 1975.
- [19] M. Bouchoucha, S. Seghour, H. Osmani and M. Bouri, *Integral Backstepping for Attitude Tracking of a Quadrotor System*, *Electronics and Electrical Engineering*, vol. 116, no. 10, pp. 75-80, 2011.
- [20] Kenichiro Nonaka and Hirokazu Sugizaki, *Integral Sliding Mode Altitude Control for a Small Model Helicopter with Ground Effect Compensation*, American Control Conference, pp. 202-207, San Francisco, CA, USA, June 29 - July 01, 2011.
- [21] Adrian-Mihail Stoica, *Automatic Flight Control Systems – Lecture Notes*, in Romanian.